

ULTRA-SHALLOW JUNCTION IMPLANT ANNEAL USING XENON ARC FLASH LAMPS

Woo Sik Yoo* and Kitaek Kang

WaferMasters, Inc., 246 East Gish Road, San Jose, CA 95112, USA

Various ultra-shallow $^{11}\text{B}^+$ and $^{49}\text{BF}_2^+$ implanted Si wafers were annealed using xenon arc flash lamps. The duration of illumination was controlled between 0.1 ms and 10 ms. Characteristics of ultra-shallow $^{11}\text{B}^+$ and $^{49}\text{BF}_2^+$ implanted Si wafers were investigated in terms of electrical activation and dopant redistribution after annealing. Sheet resistance was measured after exposure under various flash annealing conditions. Changes in dopant depth profile and crystal defect density were investigated before and after flash anneal using secondary ion mass spectroscopy (SIMS) and cross-sectional transmission electron microscopy (XTEM).

INTRODUCTION

Rapid thermal annealing (RTA) has become a preferred method for shallow junction implant annealing down to the 90 nm node [1]. Annealing times at peak temperature is often less than 1 s [2-3]. For ultra-shallow junction (USJ) formation beyond the 90 nm node, excimer laser-based and non-filament based arc lamp annealing techniques are being actively investigated due to their fast response characteristics [4-11]. The photon response time for the excimer laser and arc lamp are in the ns and ms ranges, respectively. Solid phase epitaxy (SPE) at lower temperatures (< 700 °C) after USJ implantation and epitaxial chemical vapor deposition (CVD) growth of highly doped layers are also being investigated [12-13]. As an alternate doping method, plasma doping has been actively investigated in recent years.

In an effort to extend current technology (combining ion implantation and anneal), a very rapid anneal (< 10 ms) at a very high temperature (>1100 °C) is considered the most promising solution for USJ formation to electrically activate the dopant species without causing diffusion from heating the bulk Si wafer. The combination of plasma doping and flash anneal was proposed as one of the potential solutions. Due to the high diffusivity of boron (B) in Si, p-type USJ formations pose more difficulties than n-type (P or As-based) formations. To achieve desired USJ formation, precise control of the boron implant dosage and profile, as well as proper annealing methodology, must be accomplished.

* Contact Author: e-mail: woosik.yoo@wafermasters.com, phone: +1-408-451-0856

In this study, $^{11}\text{B}^+$ (0.5 - 1.0 keV, $1.0 \sim 2.0 \cdot 10^{15}$ ions/cm²) and $^{49}\text{BF}_2^+$ (2.0 - 5.0 keV, $0.4 - 1.0 \cdot 10^{15}$ ions/cm²) implanted Si wafers with various implant energies and doses were annealed using xenon arc flash lamps.

EXPERIMENT

Due to the small size of the boron (B) atom and high diffusivity of B atoms in Si at elevated temperatures, ultra-shallow implantation without channeling and with proper boron implant anneal are critical for proper USJ formation required in electronic devices beyond the 90 nm technology node. N-type dopants (such as P and As-atoms) are relatively easy to activate without significant diffusion. A very fast heating and a very fast cool down, in the millisecond range, is desirable to form an effective USJ annealing strategy for maximum electrical activation with the least amount of dopant diffusion. High ramp-up rates can be easily achieved by supplying a large pulse of energy, but fast cooling is very difficult once the bulk wafer is heated. To meet the fast heating and cooling requirements for USJ formation, surface heating by an intense, short wavelength light pulse and fast cooling by conduction from the heated surface to the (relatively) unheated bulk Si. A very short light pulse, below a few tens of milliseconds, is required to produce a sufficiently large thermal gradient between the surface and bulk Si during the annealing cycle.

Tungsten-halogen lamps, used in conventional RTA systems, require a few seconds to reach maximum filament temperature at a given power and provide their maximum light intensity at about 1.1 μm - 1.4 μm (1.13 eV - 0.88 eV), when the filament temperature reaches approximately 3000 °C. Since the response of tungsten-halogen lamps is much too slow, they are not suitable for USJ formation applications.

Since flash lamps emit substantially shorter wavelength photons compared to both tungsten-halogen lamps and the absorption edge (0.96 μm or 1.1 eV) of Si, it is more effective in rapidly heating the surface of a Si wafer. Various types of xenon (Xe) arc lamps were used as a flash light source. The duration of the flash was controlled between 1 ms and 20 ms. By controlling the flash discharge energy in the range of 0.05 MJ \sim 0.5 MJ. Preheating of USJ implanted samples was performed up to 800 °C using a hot plate to investigate the effect of sample temperature, prior to the flash, on electrical activation and dopant diffusion. The emission spectrum of the Xe arc exhibits maximum intensity at a wavelength between 0.3 μm and 0.4 μm (4.13 eV - 3.10 eV) depending on the discharge power. The actual emission spectrum from the Xe flash lamp can be designed by selecting gas pressure and envelope material. The combination of high-energy photon irradiation and short flash time (< 100 ms) enables selective surface heating, without significant heating of the bulk Si.

Annealing characteristics of ultra-shallow $^{11}\text{B}^+$ and $^{49}\text{BF}_2^+$ implanted Si wafers with and without Ge pre-amorphization were also investigated in terms of electrical activation and dopant redistribution after annealing. Optical properties of as-implanted wafers were characterized to estimate the effect of photon energy distribution from flash lamps. Sheet resistance of implanted wafers was measured after annealing under various

flash conditions. Change in depth profiles of the implant species was investigated using secondary ion mass spectroscopy (SIMS). Solid phase re-growth and change in crystal defect density under different annealing conditions were investigated using cross-sectional transmission electron microscopy (XTEM).

RESULTS AND DISCUSSION

For successful USJ formation, both control of the as-implanted B depth profile and proper electrical activation of B with a minimum of diffusion are essential. To understand the behavior of B atoms during ion implantation, as implanted B depth profiles were measured using SIMS as the reference. The B depth profiles of $^{11}\text{B}^+$ and $^{49}\text{BF}_2^+$ implanted wafers, with and without Ge pre-amorphization, are shown in Fig. 1. BF_2 3.0 keV implanted wafers had shallower as-implanted B depth profiles than B 1.0 keV implanted wafers, regardless of Ge pre-amorphization. The Ge pre-amorphization was very effective in reducing the channeling effect during successive B or BF_2 implantations. As a result, the Ge pre-amorphized wafers have 2 ~ 3 times steeper B depth profiles than B or BF_2 implanted wafers without Ge pre-amorphization. Since the abrupt junction profile is one of the most important requirements for effective USJ formation, the Ge pre-amorphization option is very promising for controlling as-implanted junction depth.

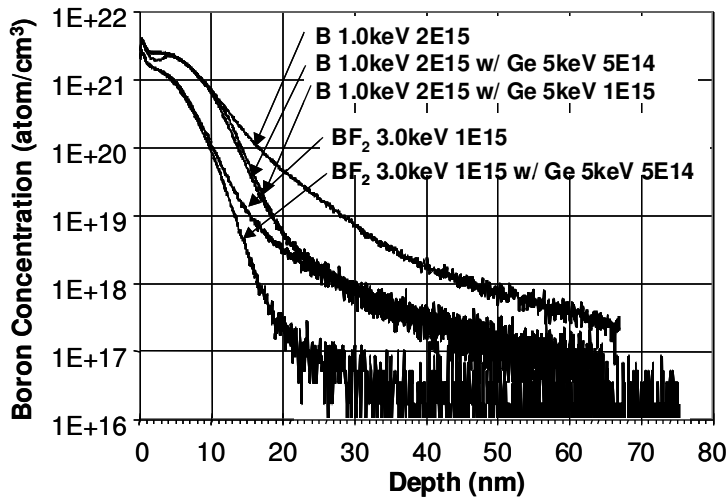


Figure 1. As implanted B depth profiles under various implant conditions.

Optical reflectance of as-implanted wafers was measured in the wavelength range of 220 - 840 nm to estimate the effect of photon energy distribution from flash lamps. The reflectance spectra of various wafers are shown in Fig. 2. Boron and BF_2 -implanted wafers with Ge pre-amorphization show lower reflectance in the ultraviolet (UV) region and higher reflectance in the visible wavelength region compared to those without Ge

pre-amorphization. The higher the reflectance, the smaller the sum of transmittance and absorbance. The absorption coefficient of photon energy in Si increases nearly exponentially, as photon energy increases, above the absorption edge ($\sim 1.0 \mu\text{m}$). To selectively heat treat the wafer surface, the use of short wavelength ($< 400 \text{ nm}$, UV region) photon energy is very important. A less reflective wafer surface, in the UV region, is ideal for USJ implant anneal using flash lamps. From the surface heating point of view, Ge pre-amorphized USJ implant wafers are expected to be more easily annealed or activated using a smaller amount of UV photon energy (power).

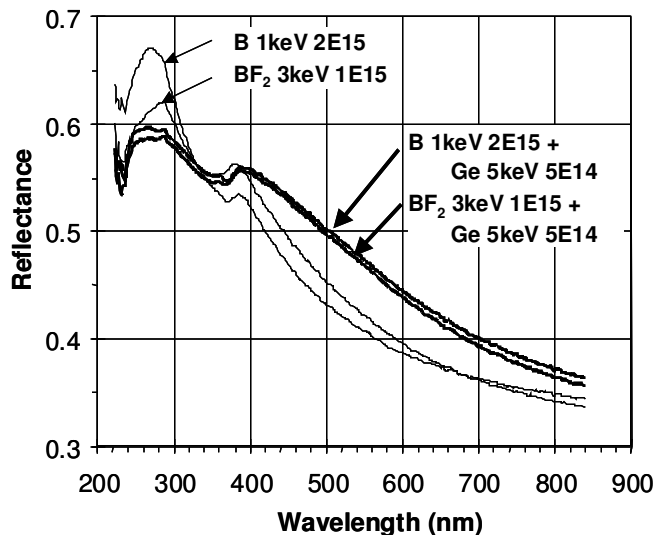


Figure 2. Optical reflectance spectra of B and BF_2 -implanted wafers before annealing in the wavelength range of 220 nm to 840 nm.

The electrical activation of $^{11}\text{B}^+$ (1 keV, $1.0 \cdot 10^{15} \text{ cm}^{-2}$) and $^{49}\text{BF}_2^+$ (3 keV, $1.0 \cdot 10^{15} \text{ cm}^{-2}$) implanted wafers with and without Ge pre-amorphization was performed using intense, short wavelength light pulses from flash lamps. The flash anneal was performed at different pre-heated wafer temperatures, from room temperature to 800 °C. The pre-heating of wafers was done using a hot plate within the process chamber. Both $^{11}\text{B}^+$ and $^{49}\text{BF}_2^+$ implanted wafers, with and without Ge pre-amorphization, showed very similar electrical activation and dopant diffusion behaviors. Since the $^{49}\text{BF}_2^+$ implanted wafers showed more abrupt B-depth profiles before annealing than did the $^{11}\text{B}^+$ implanted wafers, flash anneal results on $^{49}\text{BF}_2^+$ implanted wafers are the focus of this paper.

SIMS depth profiles of B atoms in $^{49}\text{BF}_2^+$ (3 keV, $1.0 \cdot 10^{15} \text{ cm}^{-2}$) implanted wafers without Ge pre-amorphization, both before and after flash anneal under different pre-heating temperatures, are shown in Fig. 3. Constant flash power was applied to all wafers. Only the pre-heating temperature was varied in this experiment. Sheet resistance values measured using a four-point probe were also recorded with B depth profiles. The junction

depth (x_j) has been traditionally defined as the depth at which dopant concentration equals $1.0 \cdot 10^{18} \text{ cm}^{-3}$. The as-implanted junction depth was 26.0 nm. For pre-heat temperatures of up to 400 °C, no significant B diffusion was observed. At a pre-heating temperature of 700 °C, slight B diffusion was observed. The junction depth was increased by 3.5 nm. Insufficient electrical activation was observed for pre-heating temperatures of up to 700 °C. At a pre-heat temperature of 800 °C, B diffused further into the bulk of Si after flash anneal. The junction depth was increased to 47.0 nm. The sheet resistance decreased to 307.1 Ω/\square . The optimal pre-heating temperature for this flash power level is between 700 °C and 800 °C.

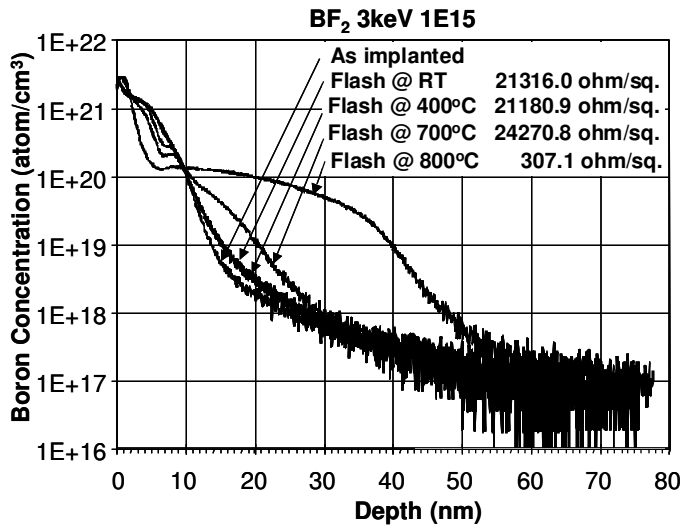


Figure 3. SIMS depth profile and sheet resistance of $^{49}\text{BF}_2^+$ (3.0 keV, $1.0 \cdot 10^{15} \text{ cm}^{-2}$ without pre-amorphization) implanted wafers before and after annealing under different pre-heating temperatures.

$^{49}\text{BF}_2^+$ (3.0 keV, $1.0 \cdot 10^{15} \text{ cm}^{-2}$) implanted wafers with Ge pre-amorphization (5.0 keV, $5.0 \cdot 10^{14} \text{ cm}^{-2}$) were annealed using flash lamps under the same annealing conditions. SIMS depth profiles of B atoms before and after flash anneal under different pre-heating temperatures are shown in Fig. 4. The as-implanted junction depth was 16.0 nm. For pre-heating temperatures below 400 °C, no significant B diffusion was observed. Again, at a pre-heat temperature of 700 °C, slight B diffusion was observed. The junction depth increased by 10.0 nm. The wafer flashed at room temperature showed a sheet resistance value of 153.6 k Ω/\square . At 400 °C pre-heat temperature, the sheet resistance was significantly reduced to 8249.5 Ω/\square . A small amount of electrical activation was observed. Sufficient electrical activation was observed at a pre-heat temperature of 700 °C. Here, a sheet resistance value of 723.1 Ω/\square was achieved at the junction depth of 26.0 nm. At a pre-heat temperature of 800 °C, a junction depth of 45.0 nm with a sheet resistance of 364.2 Ω/\square was achieved. This is substantial electrical activation. Thus, the optimal pre-heating temperature for this flash power level would appear to be between 400 °C and 800 °C.

As expected from the optical reflectance spectra, Ge pre-amorphized wafers more efficiently absorb high energy photons in the UV region than wafers without pre-amorphization. The pre-amorphization modifies the optical properties of the surface layer, independent of the presence of Ge. When Ge implantation is used for pre-amorphization, the effect of Ge in Si has to be considered. At Ge implantation conditions of 5.0 keV, $5 \cdot 10^{14}$ ions/cm², a highly Ge doped region with the maximum Ge concentration of $\sim 5.0 \cdot 10^{20}$ atoms/cm³ is formed 3 ~ 10 nm below the surface. Ge concentration in this region is almost 1.0 atomic percent of Si. As seen in SiGe alloys, the large amount of Ge incorporation, up to $5.0 \cdot 10^{20}$ atoms/cm³ in the surface layer, may have had the effect of reducing the bandgap of Si and enhancing UV absorption characteristics. To fully understand the role of pre-amorphization in USJ formation, optical property changes, before and after annealing, and atomic movement in the annealing cycle must be studied in detail. In the case of BF₂ implanted wafers, the electrical role and diffusion characteristics of F atoms should be investigated. The effect of Ge and F in pre-amorphized ¹¹B⁺ and ⁴⁹BF₂⁺-implanted wafers will be reported separately.

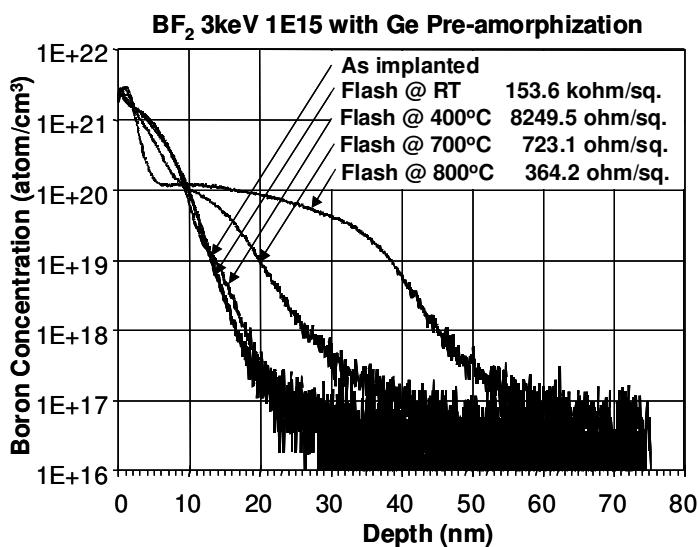


Figure 4. SIMS depth profile and sheet resistance of ⁴⁹BF₂⁺ (3.0 keV, $1.0 \cdot 10^{15}$ cm⁻²) implanted wafers with pre-amorphization (Ge 5.0 keV, $5.0 \cdot 10^{14}$ cm⁻²) before and after annealing under different pre-heating temperatures.

The sheet resistance values from ¹¹B⁺ and ⁴⁹BF₂⁺ implanted wafers with and without Ge pre-amorphization are shown in Fig. 5 as a function of junction depth (x_j) after flash anneal under various conditions. Estimated sheet resistance values of an ideal USJ with box profile are plotted as a function of carrier concentration and junction depth. In the case of the Xe-arc-lamp flash anneal performed in this study, the sheet resistance of 250 - 350 Ω/□ was achieved with a junction depth of 24.0 nm. The theoretical estimate of carrier concentration at this sheet resistance and junction depth is $\sim 2.0 \cdot 10^{20}$ cm⁻³. This carrier concentration is 2 - 3 times higher than the typical values achieved using

conventional tungsten-halogen lamp-based RTP systems. The important result is that the flash annealed wafers exhibited lower sheet resistance for a given junction depth than those annealed using conventional tungsten-halogen lamp-based RTP systems due to efficient electrical activation with less diffusion. No significant dopant diffusion was observed after Xe arc-lamp flash anneal at room temperature and low pre-heating temperatures (< 700 °C).

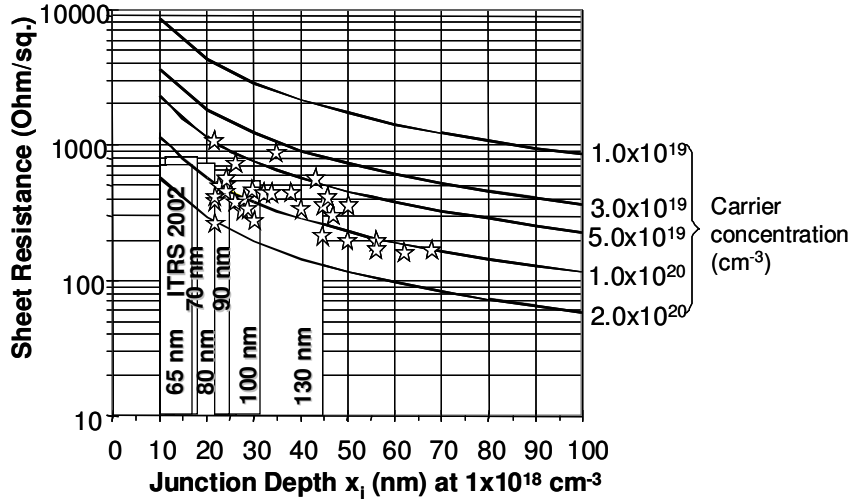


Figure 5. Sheet resistance of $^{11}\text{B}^+$ and $^{49}\text{BF}_2^+$ -implanted wafers with and without Ge pre-amorphization as a function of junction depth x_j after annealing.

Solid phase epitaxy (SPE) (or solid phase regrowth) and changes in crystal defect density under different annealing conditions were investigated using XTEM. Both Ge pre-amorphized $^{11}\text{B}^+$ and $^{49}\text{BF}_2^+$ -implanted wafers showed very similar behavior. SPE was observed for a pre-heating temperature of 500 °C. SPE is easily recognized by visual examination due to the reflectance change. The higher the SPE temperature, the lower the defect density in the junction boundary. However, even at 800 °C, the SPE was not sufficient to repair all the defects. To reduce the defect density further, more high temperature annealing is required. In fact, spike annealed wafers at 1050 °C showed almost no defects in the junction boundary. For both Ge pre-amorphized $^{11}\text{B}^+$ and $^{49}\text{BF}_2^+$ implanted wafers flash annealed at pre-heating temperature of 600 °C, significant reduction of defects was observed despite the low pre-heating temperature. Some wafers showed no defects at all. The combination of pre-heating and subsequent flash anneal is very effective in defect reduction.

Boron solid solubility in Si is strongly affected by the Si temperature. To achieve higher electrical activation, increased B solid solubility is required. A high annealing temperature is required for a fully successful USJ anneal. However, the high annealing temperature also enhances B diffusion and makes the USJ formation more problematic. A high power, short wavelength flash anneal is confirmed to be very effective in electrical

activation of fast diffusing dopants such as B without significant diffusion. Flash anneal is promising as a USJ implant anneal technique for 65 nm node and beyond.

SUMMARY

$^{11}\text{B}^+$ and $^{49}\text{BF}_2^+$ implanted Si wafers with various implant conditions (implant energy, dose and Ge pre-amorphization) were annealed using short wavelength Xe-arc flash lamps. The duration of the flash light is controlled between 1 ms and 10 ms. Annealing characteristics of ultra-shallow $^{11}\text{B}^+$ and $^{49}\text{BF}_2^+$ implanted Si wafers were investigated in terms of electrical activation and dopant redistribution after annealing. The sheet resistance and depth profile of implanted wafers were measured using a four-point probe and SIMS. Changes in crystal defect density were investigated before and after flash anneal using XTEM. Sheet resistance of 250 ~ 350 Ω/\square was achieved with a junction depth of 24.0 nm. Theoretical estimation of carrier concentration at this sheet resistance and junction depth is $\sim 2.0 \cdot 10^{20} \text{ cm}^{-3}$. The requirements for USJ implant anneal, higher electrical activation without dopant diffusion, were successfully demonstrated by the short-wavelength Xe-arc-lamp flash annealing technique combined with wafer preheating using a hotplate. Short wavelength, high-power flash annealing is very effective in electrically activating fast diffusing dopants such as B without significant diffusion and is promising as a USJ implant anneal technique for the 65 nm node and beyond.

REFERENCES

1. S. Shisiguchi, A. Mineji, T.Y. Matsuda and H. Kitajima, *Electrochem. Soc. Proc.*, **PV 99-10**, (1999) 105.
2. D. C. Jennings, G. de Cock and M. A. Foad, *Proc. 6th Int. Conf. on Advanced Thermal Processing of Semiconductors – RTP'98*, (1998) 187.
3. A. Jain, *Electrochem. Soc. Proc.*, **PV 2000-9**, (2000) 33.
4. S. Talwar, Y. Wang and C. Gelatos, *Electrochem. Soc. Proc.*, **PV 2000-9**, (2000) 95.
5. T. Gebel, M. Voelskow, W. Skorupa, G. Mannino, V. Privitera, F. Priolo, E. Naopolitani and A. Carnera, *Nucl. Instrum. Methods*, **B186** (1-4), (2002) 287.
6. R.S. Tichy, K. Elliott, S. McCoy and D. Sing, *Proc. 9th Int. Conf. on Advanced Thermal Processing of Semiconductors – RTP 2001*, (2001) 87.
7. W.S. Yoo, US Patent 6,376,806.
8. W.S. Yoo, US Patent 6,337,467.
9. T. Ito, T. Inuma, A. Murakoshi, H. Akutsu, K. Suguro, T. Arikado, K. Okumura, M. Yoshioka, T. Owada, Y. Imaoka, H. Murayama and T. Kusuda, *Jpn. J. Appl. Phys.*, **41** (2002) 2394.
10. W.S. Yoo and K. Kang, *Electrochem. Soc. Proc.*, **PV 2003-14** (2003) 111.
11. S. Talwar, D. Markle and M. Thompson, *Solid State Technology*, **46** No. 7, (2003) 83.
12. J.O. Borland, T. Matsuda and K. Sakamoto, *Solid State Technology*, **45** No. 6, (2002) 79.
13. K. Ohuchi, K. Adachi, A. Murakoshi, A. Hokazono, T. Kanemura, N. Aoki, M. Nishigohri, K. Suguro and Y. Toyoshima, *Jpn. J. Appl. Phys.*, **40** (2001) 2701.